Theoretical Studies of Methyleneamino (CH_2N) Radical Reactions. 1. Rate Constants and Product Branching Ratios for the $CH_2N + N_2O$ Process by ab Initio Molecular Orbital/ Statistical Theory Calculations

D. Chakraborty and M. C. Lin*

Department of Chemistry, Emory University, Atlanta, Georgia 30322

Received: July 27, 1998; In Final Form: December 2, 1998

High level molecular orbital calculations have been performed in the framework of the G2M method to study the kinetics and mechanism for the bimolecular reaction of CH_2N with N_2O, one of the key reactions considered in the RDX combustion modeling. Three different reaction channels have been identified for this reaction. The direct abstraction reaction, which occurs via transition state TS1 producing CH_2NO and N_2, has an activation barrier of 42.4 kcal/mol. A transition state theory calculation employing the predicted energies and molecular parameters gave rise to rate constant $k(CH_2NO) = 2.84 \times 10^{-11} \exp(-24900/T)$ cm^3/(molecule·s) in the temperature range 1000−3000 K. The $CH_2N + N_2O$ reaction can also produce CH_2N_2 and NO either by the formation and decomposition of CH_2NN_2O intermediate LM1 via TS2 and TS3 or from the cyclic intermediate LM3 via transition state TS7. LM1 can also be formed from its isomer LM2 via TS5, which appears as an additional reaction path for the formation of CH_2N_2 and NO through the same TS3 transition state. LM3 can be formed by direct side-on addition of N_2O to CH_2N via a five-membered ring transition state (TS6) with a barrier of 37.3 kcal/mol. The RRKM theory predicted the total rate constant for the formation of CH_2N_2 by these three channels: $k(CH_2N_2) = 9.93 \times 10^{-12} \exp(-22000/T)$ in the same temperature range. The cyclic intermediate (LM3) can also undergo stepwise decomposition to form endothermic products CH_2O and N_3 via TS8, intermediate LM4 and TS9; the predicted maximum barrier of this path is 32.9 kcal/mol at TS8 with respect to the reactants. The results of RRKM calculations carried out at various temperature and pressure conditions indicate that the $CH_2O + N_3$ channel is least competitive, whereas the $CH_2N_2 + NO$ channel dominates the reaction up to 2500 K.

I. Introduction

The methyleneamino radical (CH_2N) is a key reactive intermediate in the combustion of RDX $(CH_2NNO_2)_3$ and HMX $(CH_2NNO_2)_4$ in their early stages.[1−4] It may be formed directly from the fragmentation of these energetic molecules or indirectly from the decomposition of CH_2NNO_2 (methylene nitramine), the building block of RDX and HMX.

In recent kinetic simulation studies of the RDX combustion reaction by Yetter et al.[5] and Beckstead and co-workers,[6] the bimolecular reaction of CH_2N with N_2O presumably taking place by direct abstraction

$$CH_2N + N_2O \rightarrow CH_2NO + N_2$$

has been identified as one of the key processes that control the chemistry in the dark zone, the region of the flame that has a close contact with the burning surface. In the modeling calculation, the rate constant for this reaction was assumed to be $1.7 \times 10^{-13} \exp(-3000/T)$ cm^3/(molecule·s) with a relatively small activation energy (6 kcal/mol), although experimentally, the barriers for N_2O reactions with various σ radicals (including H and CH_3) are known to be very large.[7]

In view of the pivotal role assumed for the $CH_2N + N_2O$ reaction, we have carried out high-level ab initio MO calculations for its potential energy surface (PES) and performed transition-state theory (TST) and RRKM calculations for different reaction paths on the basis of the PES. The results of these calculations are reported herein.

II. Computational Methods

The geometries of the reactants, products, intermediates, and transition states have been optimized at the hybrid density functional B3LYP method[8] with the 6-311G(d,p) basis set.[9] Vibrational frequencies employed to characterize stationary points, zero-point energies (ZPE), and rate constant calculations have also been calculated at this level of theory. All the stationary points have been positively identified for local minima (number of imaginary frequencies NIMAG = 0), transition states (NIMAG = 1), or higher order top (NIMAG > 1). To confirm that the transition states connect between designated intermediates, we performed also intrinsic reaction coordinate (IRC) calculations[10] at the B3LYP/6-311G(d,p) level.

To obtain more reliable energies of various species along the PES, we used the G2M method,[11] which approaches high-level results using a series of single-point calculations for basis set size, correlation energy, and systematic error corrections. Three versions of the scheme have been suggested by Mebel et al. [11] for varying molecular sizes. For the present system with five heavy atoms, the most elaborate and computation-intensive version, G2M(RCC), was employed. The method is briefly summarized as follows.

The scheme uses B3LYP/6-311G(d,p) optimized geometries and ZPE corrections and substitutes the QCISD(T)/6-311G(d,p) calculation of the original G2 scheme[12] by the restricted open

* Corresponding author. E-mail address: chemmcl@emory.edu.

10.1021/jp983175s CCC: $18.00
Published on Web 01/15/1999

TABLE 1: Relative Energies and ZPE Corrections for Various Species through the $CH_2N + N_2O$ Reaction, Calculated at Different Levels of Theory with the B3LYP/6-311G(d,p) Optimized Geometries

species	$\langle S^2 \rangle$	ZPE	B3LYP	RCCSD(T)	G2M
$CH_2N + N_2O$	0.76, 0.00	22.7	0.0	0.0	0.0
$CH_2NN + NO$	0.00, 0.75	22.7	8.9	8.2	8.2
$CH_2NO + N_2$	0.76, 0.00	23.4	−39.1	−40.7	−38.8
$CH_2O + N_3$	0.00, 0.77	22.6	3.2	3.9	3.9
TS1	0.78	23.5	35.5	42.9	42.4
TS2	0.78	24.2	29.2	37.6	36.9
LM1(tt)	0.76	26.2	12.6	20.2	20.0
LM2(tc)	0.76	26.0	15.8	22.3	23.2
TS3	0.77	23.8	30.4	41.8	39.1
TS4	0.78	24.3	22.1	29.6	29.0
TS5	0.77	24.3	36.5	44.7	42.5
TS6	0.76	24.4	35.5	40.5	37.3
LM3	0.78	26.7	5.4	6.0	6.1
TS7	0.76	24.4	29.1	33.9	36.6
TS8	0.76	24.7	21.5	33.0	32.9
LM4	0.75	25.3	3.6	24.8	10.1
TS9	0.76	23.7	13.8	27.1	25.0

[a] The total energies (in hartree) for the $CH_2N + N_2O$ system are −278.72257, −278.05603, and −278.25867 at the B3LYP, RCCSD(T), and G2M levels of theory.

shell coupled cluster,[13] RCCSD(T)/6-311G(d,p), calculation. The total energy in G2M(RCC,MP2) is calculated as

$$E[\text{G2M(RCC,MP2)}] = E[\text{RCCSD(T)/6-311G(d,p)}] + \Delta E(+3\text{df2p}) + \Delta E(\text{HLC}) + \text{ZPE}$$

where

$$\Delta E(+3\text{df2p}) = E[\text{MP2/6-311+G(3df,2p)}] - E[\text{MP2/6-311G(d,p)}]$$

and the empirical "higher level correction"

$$\Delta E(\text{HLC,RCC,MP2}) = -0.00525 n_\beta - 0.00019 n_\alpha$$

where n_α and n_β are the numbers of α and β valence electrons, respectively.

The optimized geometries of the reactants, products, intermediates and transition states (TS) of this reaction system are shown in Figure 1, and their energies and vibrational frequencies are presented in Tables 1 and 2. The potential energy surface of the reaction is illustrated in Figure 2. All calculations were carried out with Gaussian 94[14] and MOLPRO 96[15] programs.

III. Results and Discussion

A. Ab Initio MO Calculations of the Potential Energy Surface. The reaction of CH_2N with N_2O can proceed by the approach of the CH_2N radical site to either the N or the O end of N_2O. The radical center of the CH_2N lies on the N atom, as evident from the large negative charge on the N atom and the double bond character (1.241 Å) of the CN bond. As a result, when N_2O approaches the N end, it can form a radical intermediate CH_2NN_2O, which can disproportionate to give diazomethane (CH_2N_2) and NO with endothermicity 8.2 kcal/mol at the G2M level of theory. On the other hand, the direct abstraction of the O atom of N_2O by CH_2N radical leads to the formation of methylene nitroxide (CH_2NO) and N_2, which occurs exothermically by 38.8 kcal/mol at the same G2M level of theory. CH_2N can also react with N_2O by a concerted side on addition, forming a five-membered cyclic ring intermediate (LM3), leading to the formation of CH_2O and N_3 as other possible products of this reaction; the endothermicity for the formation of $CH_2O + N_3$ is 3.9 kcal/mol at the G2M level of theory.

Channel Forming CH_2NO and N_2. The only bimolecular reaction of CH_2N with N_2O considered in the kinetic simulation of the RDX combustion reaction[5,6] is the formation of the exothermic products CH_2NO and N_2 through the direct abstraction of the oxygen of N_2O by the CH_2N radical. The abstraction of the O atom from N_2O takes place via the transition structure TS1, whose barrier is 42.4 kcal/mol at the G2M level and 42.9 and 35.5 kcal/mol at the CCSD and B3LYP levels of theory, respectively. TS1 is an early transition state with planar structure (C_s; $^2A'$), having an imaginary frequency of 765 cm^{-1}. The forming NO bond in TS1 is 1.753 Å and the dissociating NO bond is elongated by 0.16 Å from isolated N_2O. IRC calculation in both reactants and products directions indicate that TS1 connects both the reactants and the products along this reaction path. The product CH_2NO radical also possesses a planar structure (C_s; $^2A'$) with CN and NO bond distances of 1.279 and 1.218 Å, respectively, and the CNO bond angle of 135.1°. Since this reaction channel has the highest activation barrier

TABLE 2: Vibrational Frequencies and Moments of Inertia for All Species

species	I_i (amu)	ν_i (cm^{-1})
CH_2N	6.3, 45.9, 52.2	932, 989, 1379, 1722, 2955, 3007
N_2O	142.6, 142.6	608, 608, 1338, 2356
CH_2NN	6.5, 158.9, 165.4	426, 442, 580, 1116, 1213, 1436, 2205, 3182, 3305
NO	35.2, 35.2	1989
CH_2NO	14.1, 153.3, 167.3	460, 700, 815, 1130, 1251, 1489, 1724, 3105, 3255
N_2	30.0, 30.0	2447
CH_2O	6.3, 46.2, 52.6	1202, 1270, 1539, 1826, 2868, 2917
N_3	138.8, 138.8	491, 591, 1374, 1723
TS1	79.2, 587.3, 666.5	765i,[a] 57, 179, 377, 407, 579, 601, 960, 1023, 1084, 1398, 1716, 1882, 3032, 3113
TS2	40.1, 730.9, 771.0	705i, 77, 212, 384, 443, 621, 642, 1043, 1090, 1212, 1406, 1699, 1919, 3042, 3126
LM1	30.6, 659.3, 689.9	130, 277, 357, 533, 609, 788, 990, 1040, 1192, 1328, 1449, 1633, 1695, 3078, 3208
LM2	72.7, 530.6, 603.4	87, 222, 470, 507, 720, 752, 868, 1054, 1177, 1281, 1437, 1640, 1703, 3076, 3193
TS3	39.4, 744.2, 773.2	363i, 118, 206, 230, 404, 598, 633, 766, 1118, 1186, 1492, 1725, 1837, 3093, 3222
TS4	76.2, 612.8, 689.1	578i, 71, 172, 391, 523, 635, 646, 1040, 1081, 1255, 1406, 1701, 1917, 3036, 3117
TS5	49.3, 630.4, 648.9	549i, 120, 188, 419, 650, 668, 833, 956, 1091, 1202, 1403, 1554, 1585, 3094, 3227
TS6	186.9, 263.6, 438.1	530i, 196, 314, 583, 584, 717, 805, 954, 1022, 1223, 1325, 1445, 1802, 3016, 3091
LM3	184.3, 190.4, 363.1	309, 596, 812, 859, 926, 949, 975, 983, 1057, 1136, 1232, 1338, 1454, 3007, 3046
TS7	188.6, 257.7, 433.9	457i, 210, 276, 312, 588, 674, 810, 949, 1092, 1171, 1432, 1478, 1791, 3105, 3204
TS8	179.2, 244.6, 412.2	435i, 281, 571, 649, 691, 805, 823, 1075, 1098, 1211, 1258, 1337, 1734, 2858, 2866
LM4	127.2, 452.2, 568.3	58, 164, 466, 558, 686, 766, 850, 1123, 1128, 1239, 1300, 1370, 2252, 2857, 2863
TS9	143.0, 484.9, 615.0	630i, 89, 146, 425, 540, 639, 724, 968, 1112, 1324, 1366, 1516, 2020, 2763, 2974

[a] i stands for imaginary frequency.

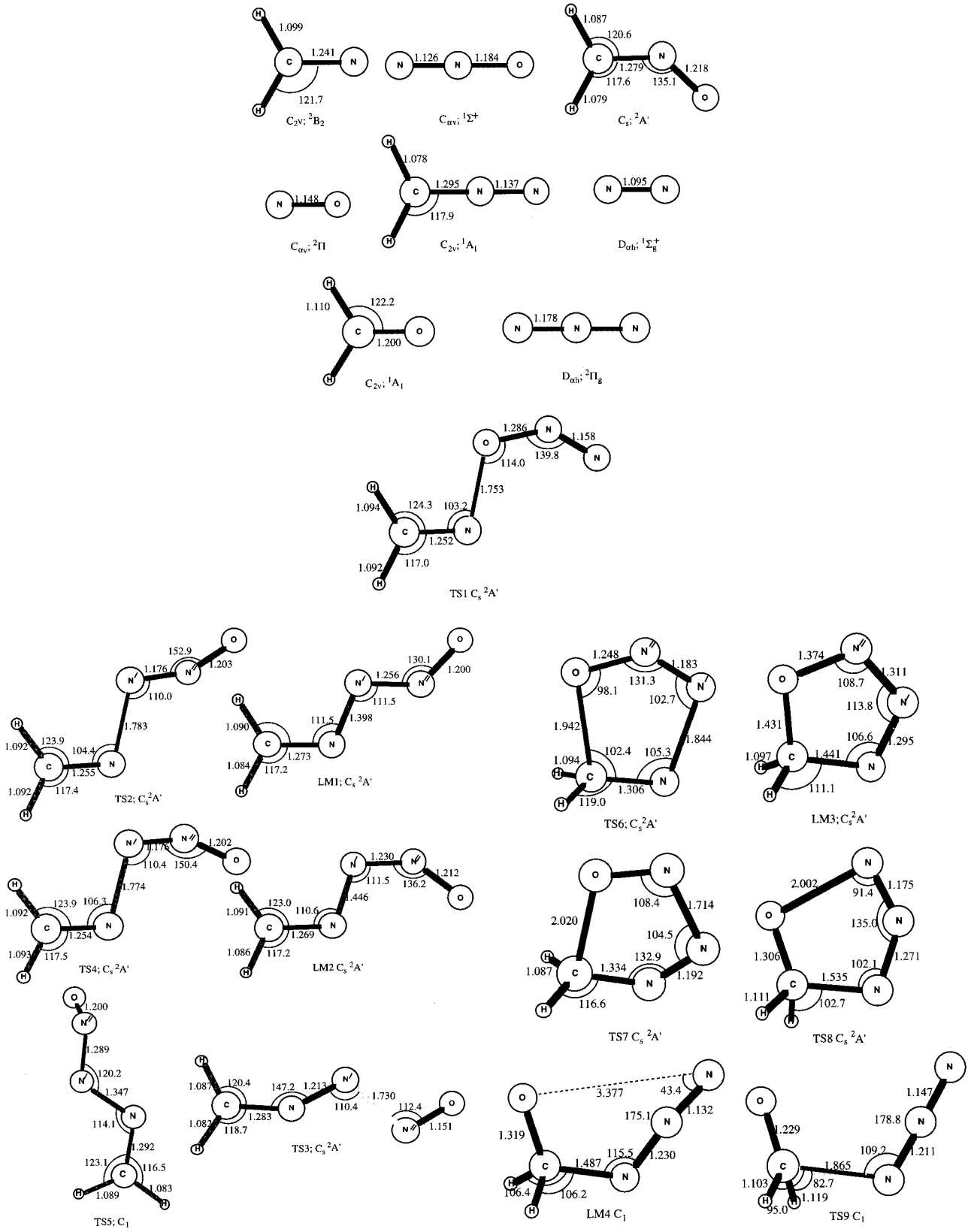

Figure 1. Optimized geometries of reactants, products, intermediates, and transition states at the B3LYP/6-311g(d,p) level of theory.

along the PES, the exothermic products $CH_2NO + N_2$ are unlikely to be formed favorably over the other possible products in the bimolecular reaction of CH_2N with N_2O.

Channel Forming CH_2N_2 and NO. The initial association of the CH_2N with N_2O to form the $CH_2NN'N''O$ radical intermediate can only take place through some association barrier, as commonly observed in the reaction of N_2O with other σ radicals. The most stable structure (LM1) of this radical intermediate has a planar (C_s, $^2A'$) structure with a trans−trans (tt) orientation of the N′N″ and N″O bonds with respect to CN and NN′ bonds. The formation of LM1 is endothermic by 20.0 kcal/mol at the G2M level of theory; it is controlled by the initial transition state TS2, whose barrier is 36.9 kcal/mol at the G2M level and 37.6 and 29.2 kcal/mol at CCSD(T) and B3LYP levels of theory.

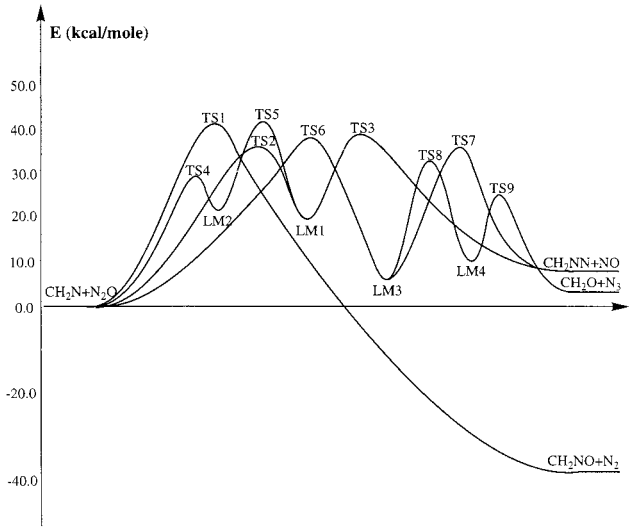

Figure 2. Potential energy profile for the reaction $CH_2N + N_2O$ based on the G2M method.

The CN bond in LM1 (1.273 Å) has a more double bond character and is lengthened by 0.03 Å with respect to the CN bond in the CH_2N radical. The NN′ bond in LM1 (1.398 Å) is of more single bonded nature whereas the N′N″ bond (1.256 Å) has a more double bond character. As a consequence, the radical center in LM1 lies more on the N″ atom, which is also evident from the Mulliken charges on different atomic centers (C = 0.199, N = −0.147, N′ = −0.113, N″ = 0.241, and O = −0.181).

The intermediate LM1 can have other possible rotational isomers, namely trans−cis (tc) and cis−cis (cc), by the rotation around the N′N″ bond. Our calculation reveals that the cc isomer is not a real minimum in the potential energy surface (PES). The search for the cc isomer always converged to the tc (LM2) isomer, indicating that there is no stable intermediate with cc conformation along the PES. The tc isomer (LM2) is a stable one and can be formed directly via another initial transition state (TS4), the barrier of which is 22.1, 29.6, and 29.0 kcal/mol at B3LYP, CCSD(T), and G2M levels of theory, respectively. As alluded to above, LM1 is endothermic by 20.0 kcal/mol with respect to the reactants at the G2M level, whereas its isomer LM2 is 3.2 kcal/mol less stable than this at the same level of theory. The transition states TS2 and TS4 have a similar type of structure (C_s; $^2A'$) with the forming NN′ bond distances of 1.783 and 1.774 Å, respectively. At the B3LYP level of theory both TS2 and TS4 are intermediate transition states with N′N″O angles of 152.9 and 150.4°, respectively, and with N′N″ and N″O bond lengths between isolated N_2O and their respective intermediates. The more stable isomer LM1 can then be reached from LM2 by the rotation around the N′N″ bond. Since the N′N″ bond in both LM1 and LM2 has more double bond character, this isomerization involves a large transition barrier. At the G2M level of theory TS5 has an energy of 42.5 kcal/mol with respect to the reactants. LM1 can dissociate into diazomethane (CH_2N_2) and NO through the transition state TS3, whose barrier is 19.1 kcal/mol at the G2M level of theory. The large barrier results from the breaking of the N′N″ double bond in this dissociation process. TS3 has a planar structure (C_s; $^2A'$) with the dissociating N′N″ bond distance of 1.73 Å and the CNN′ angle approaching more toward linearity, as in diazomethane, changing from 111.5° in LM1 to 147.2° in TS3.

The endothermic $CH_2N_2 + NO$ products can also be reached through a different reaction path via the formation and decomposition of a cyclic intermediate LM3, as shown in Figure 2. LM3 is a cyclic form of the other possible (cc) conformation of LM1 and LM2. LM3 is a five-membered oxyring type intermediate with C_s ($^2A'$) symmetry and can be more favorably formed by the direct side-on addition of N_2O on CH_2N through transition state TS6. TS6 has a planar structure (C_s) with cis−cis orientation of the N′N″ and N″O bonds and having an imaginary frequency of 530 cm^{-1}. The forming NN′ and CO bonds in TS6 are 1.85 and 1.95 Å, respectively, and both the hydrogens of CH_2 have an intermediate orientation between their planar and cyclic forms. TS6 is energetically 37.3 kcal/mol higher than the reactants at the G2M level of theory and 35.5 and 40.5 kcal/mol higher at B3LYP and CCSD(T) levels. Intermediate LM3 is 6.1 kcal/mol more endothermic than the reactants, 13.9 kcal/mol more stable than LM1, and 17.1 kcal/mol more stable than LM2 at the G2M level of theory. LM3 can undergo isomerization to form LM4, a potential precursor of the $CH_2O + N_3$ products (vide infra), and dissociation to produce $CH_2N_2 + NO$ via the transition state TS7, whose barrier is 36.6, 29.1, and 33.9 kcal/mol at the G2M, B3LYP, and CCSD(T) levels, respectively. TS7 is a late transition state with dissociating N′N″ and CO bond lengths of 1.714 and 2.020 Å, respectively. As this reaction channel has a similar activation barrier compared to the other described above, the formation of $CH_2N_2 + NO$ might be equally favorable through these reaction channels. Since both reaction channels are controlled by large activation barriers, it is unlikely that these products are reached through these reaction channels except at very high temperatures.

Channel Forming CH_2O and N_3. The formation of CH_2O and N_3 in the bimolecular reaction of CH_2N and N_2O is more complicated and can only take place by a stepwise mechanism through the O migration from the cyclic LM3 intermediate. As indicated above, LM3 can go through TS8 to another stable intermediate LM4 by the cleavage of the NO bond. An IRC calculation along the reaction path confirms that TS8 connects LM3 with LM4. TS8 is a late transition state with the CN bond distance of 1.535 Å and the dissociating NO bond distance of 2.002 Å. At the G2M level TS8 is 26.8 kcal/mol higher than LM2 and 16.1 and 27.0 kcal/mol higher at the B3LYP and CCSD(T) levels of theory. LM4 has an acyclic structure of C_1 symmetry with a CN bond distance of 1.487 Å. LM4 is endothermic by 10.1 kcal/mol with respect to the reactants at the G2M level but 4.0 kcal/mol less stable than LM3 at the same level of calculation. The N_3 fragment in LM4 is close to linearity with an NN′N″ bond angle of 175.1°, and both the NN bond distances are closer to those of the isolated N_3 radical. The CO bond in LM4 has an intermediate bond length of 1.319 Å, and the CH_2O fragment still deviates from coplanarity. LM4 can undergo dissociation of the CN single bond via the transition state TS9 to the CH_2O and N_3 products, which are endothermic by 3.2 kcal/mol at the B3LYP level and 3.9 kcal/mol at both CCSD(T) and G2M levels of theory. TS9 is a very late transition state with the dissociating CN bond distance of 1.865 Å and both the dissociating fragments, CH_2O and N_3 structurally very similar to their isolated forms. TS9 has an activation barrier of 14.9 kcal/mol over LM4 at the G2M level of theory. Thus it is evident from this calculation that the endothermic products CH_2O and N_3, can be formed by the direct formation of the cyclic LM3 intermediate from the reactants followed by its dissociation through a high-energy reaction path. As the rate-controlling steps of the formation and decomposition of cyclic intermediate LM3 has a high activation barrier, the endothermic products CH_2O and N_3 in the reaction of CH_2N and N_2O can only be reached at very high temperatures. From the calculated

G2M potential energy profile for the three sets of products, it is clearly evident that both reaction paths leading to the formation of $CH_2N_2 + NO$ and $CH_2O + N_3$ have a comparable activation barrier along the PES and, hence, might be considered as favorable products of this bimolecular reaction.

B. TST and RRKM Calculations of Rate Constants. As discussed in the preceding section, the three sets of reaction products, $CH_2NO + N_2$, $CH_2N_2 + NO$, and $CH_2O + N_3$, can be formed by four reaction paths. The rate constants associated with these paths should be calculated individually. For $CH_2N_2 + NO$, which can be formed by three different pathways, the total rate constant is the sum of individual rate constants. In our rate constant calculations, we employ the transition state theory (TST) for the direct abstraction process and the Rice−Ramsperger−Kassel−Marcus (RRKM) theory for the processes occurring via long-lived intermediates using the G2M(RCC,-MP2) energies given in Table 1 and the B3LYP/6-311G(d,p) molecular parameters and frequencies presented in Table 2.

$CH_2NO + N_2$. For the abstraction reaction channel leading to CH_2NO and N_2

$$CH_2N + N_2O \xrightarrow{TS1} CH_2NO + N_2 \qquad (1)$$

a TST calculation for the 1000−3000 K temperature range gave rise to the expression

$$k_1 = 2.84 \times 10^{-11} \exp(-24900/T)\ \mathrm{cm^3/(molecule{\cdot}s)}$$

$CH_2N_2 + NO$. As mentioned in the previous section, the $CH_2N_2 + NO$ products can be reached by three different reaction paths:

$$CH_2N + N_2O \overset{TS2}{\rightleftharpoons} LM1 \overset{TS3}{\rightleftharpoons} CH_2N_2 + NO \qquad (2a)$$

$$CH_2N + N_2O \overset{TS4}{\rightleftharpoons} LM2 \overset{TS5}{\rightleftharpoons} LM1 \xrightarrow{TS3} CH_2N_2 + NO \qquad (2b)$$

$$CH_2N + N_2O \overset{TS6}{\rightleftharpoons} LM3 \xrightarrow{TS7} CH_2N_2 + NO \qquad (2c)$$

We apply here our different versions of multichannel RRKM programs[16,17] to calculate the rate constants for these channels. Reaction channels 2a and 2b are actually coupled through the stable intermediate LM1. Accordingly, in the reaction 2a calculation we included the loss of LM1 by TS5, whereas for reaction channel 2b, we included the disappearance of LM1 by TS2 to obtain the net formation rate of $CH_2N_2 + NO$ through this reaction path. Similarly, in the channel 2c calculation, the loss of LM3 by TS8 is also included. The calculated rate constants for these channels in the temperature range of 1000−3000 K in units of $cm^3/(molecule{\cdot}s)$ are

$$k_{2a} = 8.92 \times 10^{-12} \exp(-21900/T)$$

$$k_{2b} = 2.02 \times 10^{-12} \exp(-25100/T)$$

$$k_{2c} = 3.98 \times 10^{-14} \exp(-24900/T)$$

$$k_2 = k_{2a} + k_{2b} + k_{2c} = 9.93 \times 10^{-12} \exp(-22000/T)$$

It is evident from these calculated rate constants that the formation of $CH_2N_2 + NO$ is dominated by reaction channel 2a and only at very high temperatures would other channels become accessible. The results of the calculation indicated that the predicted rate constants are pressure independent in the range of 10 Torr to 200 atm. For coupled channels 2a and 2b, for example, the rates of deactivation of the activated intermediates

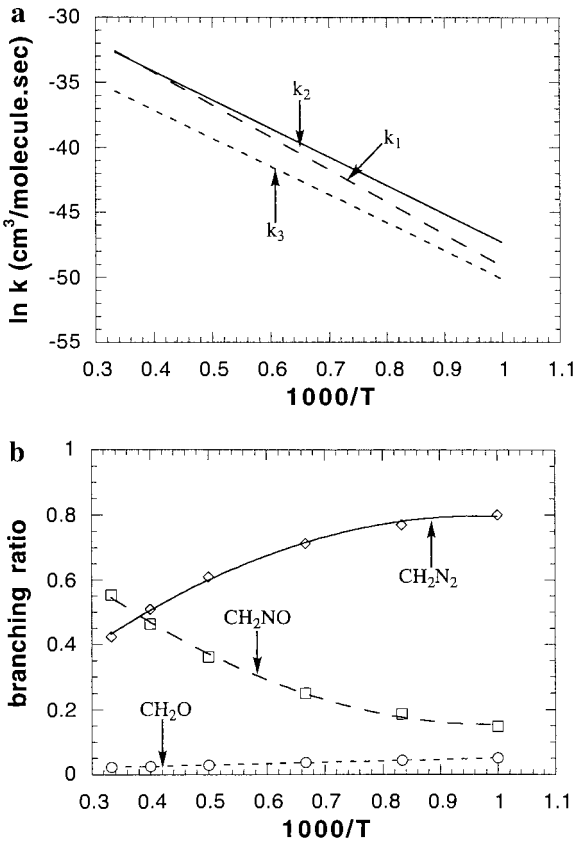

Figure 3. (a) Arrhenius plots for the bimolecular rate constants for the formation of $CH_2NO + N_2$, $CH_2N_2 + NO$, and $CH_2O + N_3$ through reaction channels 1, 2, and 3 in the temperature range 1000−3000 K. (b) Temperature dependence of the product branching ratios through the individual channels 1, 2, and 3.

to the potential wells LM1 and LM2 are significantly less important compared to their rates of disproportionation through the individual product channels. Figure 3a shows the overall rate of formation of $CH_2N_2 + NO$ through all these individual channels along with the rate constants for formation of $CH_2NO + N_2$ and $CH_2O + N_3$ to be discussed below. At higher temperatures, the rates of formation of CH_2NO and CH_2N_2 become comparable although at lower temperatures the formation rate of CH_2NO is much less due to the presence of a higher activation barrier for this process.

$CH_2O + N_3$. The reaction channel leading to the formation of CH_2O and N_3

$$CH_2N + N_2O \xrightarrow{TS6} LM3 \xrightarrow{TS8} LM4 \xrightarrow{TS9} CH_2O + N_3 \qquad (3)$$

is connected with channel 2c, as mentioned above. Our coupled dual channel RRKM calculation (incorporating the loss of LM3 by TS7) yielded the bimolecular formation rate constants for (3) at the same temperature and pressure ranges:

$$k_3 = 4.58 \times 10^{-13} \exp(-21800/T)\ \mathrm{cm^3/(molecule{\cdot}s)}$$

This result, presented in Figure 3a for comparison with k_1 and k_2, is also pressure independent in the same range as mentioned above. As evident from the figure, the rate of formation of $CH_2O + N_3$ through reaction channel 3 is less important compared to the other individual channels, i.e., (1) and (2).

Product Branching Ratios. The product branching ratio through each individual channel is calculated by k_i/k_t where the total rate constant k_t for the three product channels is obtained

by summing the individual rate constants ($k_1 + k_2 + k_3$). Figure 3b presents the temperature dependence of the calculated branching ratios in the same range of temperature (1000−3000 K).

Estimate of Errors. For practical applications, one would like to ascertain the reliability of the computed rate constants. Previously, we have shown that the G2M(RCC,MP2) scheme[11] predicted the rate constant for $C_2H_3 + O_2$ quantitatively,[17] while the simpler version G2M(rcc,MP2)[11] also predicted reliably (within ±1 kcal/mol in comparison with experiment) the first C−H bond dissociation energies of C_6H_6[18] and C_6H_5[19] as well as the rate constant for the $C_6H_5 + H_2 \rightarrow C_6H_6 + H$ metathetical reaction.[18,20] For the present five heavy-atom system, the direct abstraction reaction 1 with a likely error in the predicted activation energy, ±2 kcal/mol (which may be somewhat bigger or smaller depending on the extent of error propagation or cancelation between the reactants and the TS), has a possible error in the absolute rate constant at combustion temperatures, $\Delta k_1(2000\ \mathrm{K}) \approx \pm 50\%$. Possible errors for k_2 and k_3, evaluated by multichannel RRKM calculations are harder to assess. If the complex $C_2H_3 + O_2$ reaction (which has as many as five product channels) can be used as a guide, the absolute error estimated above may be also reasonable for the two indirect metathetical processes.

IV. Concluding Remarks

The results of our ab initio MO calculations employing the G2M method reveal the possibility of three different product channels for the bimolecular reaction taking place between CH_2N and N_2O. The direct abstraction reaction was found to occur by a distinct transition state TS1 with a barrier of 42.4 kcal/mol, producing CH_2NO and N_2. On the other hand, both the endothermic $CH_2N_2 + NO$ and $CH_2O + N_3$ products can be reached only by stepwise mechanisms via the formation and decomposition of some radical intermediates. The former product pair can be formed by three different reaction paths: the first path takes place by the formation and decomposition of the CH_2NN_2O (LM1) intermediate via TS2 and TS3, the maximum barrier of which is 39.1 kcal/mol with respect to the reactants; the second path occurs by the formation of LM1 from its isomer LM2 via TS4 and TS5 followed by disproportionation by the same TS3; the third path goes through the formation of a cyclic oxyring type intermediate (LM3) and its disproportionation to the products, whose maximum barrier is 37.3 kcal/mol. The latter is significantly affected by the decomposition LM3 in a stepwise manner, which has the maximum barrier of 32.9 kcal/mol at TS8 with respect to the reactants, leading to the formation of $CH_2O + N_3$ via LM4. Since all the three reaction channels are controlled by high-energy activation barriers of the respective steps, none of these products are expected to be reached at ambient temperature, whereas at elevated temperatures the formation of CH_2N_2 and NO is relatively more favorable. The rate constants for these three processes have been calculated with the help of the transition state theory or the RRKM theory, wherever applicable, and are recommended for the kinetic modeling of RDX combustion at high temperatures.

Acknowledgment. The authors gratefully acknowledge the support of this work by the Caltech MURI project under ONR grant NO. N00014-95-1338, Drs. R. S. Miller and J. Goldwasser, program managers. We thank the Cherry L. Emerson Center for Scientific Computation for the use of computing facilities and various programs. We also thank one of the referees for suggesting the possible existence of TS6, which we failed to find initially.

References and Notes

(1) Alexander, M. H.; Dagdigian, P. J.; Jacox, M. E.; Kolb, C. E.; Melius, C. F.; et al. *Prog. Energy Combust. Sci.* **1991**, *17*, 263.

(2) Adams, G. F.; Shaw, R. W., Jr. *Annu. Rev. Phys. Chem.* **1992**, *43*, 311.

(3) Zhao, X.; Hintsa, E. J.; Lee, Y. T. *J. Chem. Phys.***1988**, *88*, 801.

(4) Melius, C. F. Thermochemical Modeling: II. Application to Ignition and Combustion of Energetic Materials. *Chemistry and Physics of Energetic Materials*; Bulusu, S. N., Ed.; 1990; pp 51−78.

(5) Prasad, K.; Yetter, R. A.; Smooke, M. D. *Combust. Sci. Technol.* **1997**, *124*, 35.

(6) (a) Davidson, J. E.; Beckstead, M. W. *J. Propul. Power* **1997**, *13*, 375. (b) Davidson, J. E.; Beckstead, M. W.; Erikson, W.; Jing, Q. CPIA Pub. No. 638; CPIA: Laurel, MD, 1995; Vol. I, p 41.

(7) Mallard, W. G.; Westley, F.; Herron, J. T.; Hampson, R. F. NIST Chemical Kinetics Database − Version 6.01; NIST Standard Reference Data; NIST: Gaithersburg, MD 1994.

(8) (a) Becke, A. D. *J. Chem. Phys.* **1993**, *98*, 5648. (b) *Ibid.* **1992**, *96*, 2155. (c) *Ibid*. **1992**, *97*, 9173. (d) Lee, C.; Yang, W.; Parr, R. G. *Phys. Rev. B* **1988**, *37*, 785.

(9) Hehre, W. J.; Radom, L.; Schleyer, P. v. R.; Pople, J. A. *Ab Initio Molecular Orbital Theory*; Wiley: New York, 1986.

(10) Gonzalez, C.; Schlegal, H. B. *J. Chem. Phys.* **1989**, *90*, 2154.

(11) Mebel, A. M.; Morokuma, K.; Lin, M. C. *J. Chem. Phys.* **1995**, *103*, 7414.

(12) (a) Curtiss, L. A.; Raghavachari, K.; Trucks, G. W.; Pople, J. A. *J. Chem. Phys.* **1991**, *94*, 7221. (b) Pople, J. A.; Head-Gordon, M.; Fox, D. J.; Raghavachari, K.; Curtiss, L. A. *Ibid.* **1989**, *90*, 5622. (c) Curtiss, L. A.; Jones, C.; Trucks, G. W.; Raghavachari, K.; Pople, J. A. *Ibid.* **1990**, *93*, 2537.

(13) (a) Purvis, G. D.; Bartlet, R. J. *J. Chem. Phys.* **1982**, *76*, 1910. (b) Hampel, C.; Peterson, K. A.; Warner, H.-J. *Chem. Phys. Lett.* **1992**, *190*, 1. (c) Knowels, P. J.; Hampel, C.; Warner, H.-J. *J. Chem. Phys.* **1994**, *99*, 5219. (d) Degan, M. J. O.; Knowels, P. J. *Chem. Phys. Lett* **1994**, *227*, 321.

(14) Frisch, M. J.; Trucks, G. W.; Schlegal, H. B.; Gill, P. M. W.; Johnson, B. G.; Robb, M. A.; Cheeseman, J. R.; Keith, T.; Petersson, G. A.; Montgomery, J. A.; Raghavachari, K.; Al-Laham, M. A.; Zakrzewiski, V. G.; Ortiz, J. V.; Foresman, J. B.; Cioslowski, J.; Stefanov, B. B.; Nanayakkara, A.; Challacombe, M.; Peng, C. Y.; Ayala, P. Y.; Chen. W.; Wong, M. W.; Andres, J. L.; Replogle, E. S.; Gomperts, R.; Martin, R. L.; Fox, D. J.; Binkley, J. S.; Defrees, D. J.; Baker, J.; Stewart, J. P.; Head-Gordon, M.; Gonzalez, C.; Pople, J. A. GAUSSIAN 94, Revision B.2; Gaussian, Inc.; Pittsburgh, PA, 1995.

(15) MOLPRO is a package of ab initio programs written by H.-J. Werner, and P. J. Knowels, with contributions from J. Almlöf, R. D. Amos, M. J. O. Deegan, S. T. Elbert, C. Hampel, W. Meyer, K. Peterson, R. Pitzer, A. J. Stone, P. R. Taylor, and R. Lindh.

(16) Diau, Eric W. G.; Lin, M. C. *J. Phys. Chem.* **1995**, *99*, 6589.

(17) Mebel, A. M.; Diau, E. G. W.; Lin, M. C.; Morokuma, K. *J. Am. Chem. Soc.* **1996**, *118*, 9759.

(18) Mebel, A. M.; Lin, M. C.; Yu, T.; Morokuma, K. *J. Phys. Chem. A* **1997**, *101*, 3189.

(19) Madden, L. K.; Moskaleva, L. V.; Kristyan, S.; Lin, M. C. *J. Phys. Chem. A* **1997**, *101*, 6790.

(20) Park, J.; Dyakov, I. V.; Lin, M. C. *J. Phys. Chem. A* **1997**, *101*, 8839.